

---

---

# Diagnostic Accuracy of $^{99m}\text{Tc}$ -Sestamibi SPECT/CT for Characterization of Solid Renal Masses

Ashwin Singh Parihar<sup>\*1</sup>, Joyce Mhlanga<sup>\*1,2</sup>, Carrie Ronstrom<sup>2,3</sup>, Lisa R. Schmidt<sup>1</sup>, Robert S. Figenshau<sup>2,3</sup>, Farrokh Dehdashti<sup>\*1,2</sup>, and Richard L. Wahl<sup>\*1,2</sup>

<sup>1</sup>Mallinckrodt Institute of Radiology, Washington University School of Medicine, St. Louis, Missouri; <sup>2</sup>Siteman Cancer Centre, Washington University School of Medicine, St. Louis, Missouri; and <sup>3</sup>Division of Urology, Department of Surgery, Washington University School of Medicine, St. Louis, Missouri

---

Our objective was to assess the diagnostic accuracy of  $^{99m}\text{Tc}$ -sestamibi SPECT/CT for characterizing solid renal masses. **Methods:** Imaging and clinical records of patients who underwent  $^{99m}\text{Tc}$ -sestamibi SPECT/CT for clinical work-up of their solid renal masses from September 2018 to October 2021 were retrospectively reviewed. Histopathology formed the reference standard, and the diagnoses were categorized as malignant/concerning (renal cell carcinomas [RCCs] other than chromophobe histology) and benign/nonconcerning (oncocytic tumors including chromophobe RCC, other benign diagnoses) to calculate the sensitivity and specificity of  $^{99m}\text{Tc}$ -sestamibi SPECT/CT and contrast-enhanced CT (ceCT). The clinical reads of the SPECT/CT images were used for visual classification of the lesions. Additionally, the SPECT images were manually segmented to obtain the maximum and mean counts of the lesion and adjacent renal cortex and maximum and mean lesion Hounsfield units. **Results:**  $^{99m}\text{Tc}$ -sestamibi SPECT/CT was performed on 42 patients with 62 renal masses. A histopathologic diagnosis was available for 27 patients (18 male, 9 female) with 36 solid renal masses. ceCT findings were available for 20 of these patients. The most commonly identified single histologic type was clear cell RCC (13/36; 36.1%). Oncocytic tumors were the most common group of nonconcerning lesions (15/36), with oncocytoma as the predominant histologic type ( $n = 6$ ). The sensitivity and specificity of SPECT/CT for diagnosing a nonconcerning lesion were 66.7% and 89.5%, respectively, compared with 10% and 75%, respectively, for ceCT. The lesion-to-kidney ratios for maximum and mean counts and maximum lesion Hounsfield units showed significant differences between the 2 groups ( $P < 0.05$ ). The lesion-to-kidney mean count ratio at a cutoff of 0.46 showed a sensitivity and specificity of 87.5% and 86.67%, respectively, for detecting nonconcerning lesions, which was significantly higher than that of ceCT. **Conclusion:** The current literature on the utility of  $^{99m}\text{Tc}$ -sestamibi SPECT/CT for characterization of solid renal masses is limited. We offer additional evidence of the incremental value of  $^{99m}\text{Tc}$ -sestamibi SPECT/CT over ceCT for differentiating malignant or aggressive renal tumors from benign or indolent ones, thereby potentially avoiding overtreatment and its associated complications. Quantitative assessment can further increase the diagnostic accuracy of SPECT/CT and may be used in conjunction with visual interpretation.

**Key Words:**  $^{99m}\text{Tc}$ -sestamibi; MIBI; SPECT/CT; oncocytoma; chromophobe; renal cell carcinoma

**J Nucl Med 2023; 64:90–95**  
DOI: 10.2967/jnumed.122.264329

The widespread use of cross-sectional imaging has led to an increased incidental detection of renal masses (1). Solid renal masses form a diagnostic challenge because conventional imaging with CT or MRI cannot reliably differentiate benign and indolent tumors from the more aggressive ones (2). Most of these tumors are malignant, with clear cell renal cell carcinoma (RCC) forming the most common histologic type, and around 10%–20% are benign (3). The situation gets more complex with incidentally detected small renal masses ( $\leq 4$  cm) that are consistent with a clinical stage T1a RCC. These tumors were historically managed with universal radical nephrectomy. However, it was recognized that the prognosis for patients with small renal masses is favorable, and a significant proportion of these patients can be managed with active surveillance (4,5). Further, among the 80% of these small renal masses that are malignant, only 20% are high-grade or locally invasive. The remaining majority have limited metastatic potential, including tumors such as chromophobe RCC (4,6).

The current recommendation for managing a small renal mass is to perform a biopsy whenever it is likely to change management and to perform a partial nephrectomy as the standard treatment whenever indicated (7). However, renal biopsy has technical challenges, including an approximately 20% nondiagnostic rate and a limited ability to differentiate low-grade from high-grade tumors (8–10). It is therefore clinically relevant and meaningful for a diagnostic test to not only distinguish benign from malignant tumors but also differentiate indolent tumors from aggressive ones. This ability can help in potentially avoiding overtreatment in patients with relatively indolent tumors while appropriately managing the more aggressive malignancies.

$^{99m}\text{Tc}$ -sestamibi is a lipophilic radiotracer that preferentially localizes in mitochondria-rich cells. Benign and indolent renal tumors such as oncocytic neoplasms and chromophobe RCC are mitochondria-rich and typically avid on  $^{99m}\text{Tc}$ -sestamibi SPECT/CT, compared with clear cell RCC and other aggressive tumors, which are typically nonavid (11). In addition, aggressive RCCs have a high multidrug-resistance-pump expression that leads to active efflux of  $^{99m}\text{Tc}$ -sestamibi, thus contributing to negligible tracer retention (12). Prior studies have shown the effectiveness of  $^{99m}\text{Tc}$ -sestamibi in distinguishing oncocytic tumors from high-grade RCC (11,13–16). However, the data are still relatively sparse in terms of limited unique patient populations and the variety of benign and malignant histologies. A recent systematic review reported on 4 articles and mentioned the limited number of included studies as a major drawback (17). Additionally, there has been limited emphasis on the quantitative aspects of SPECT/CT, including parameters from both the SPECT and the CT components of the study.  $^{99m}\text{Tc}$ -sestamibi SPECT/CT is not yet

---

Received Apr. 22, 2022; revision accepted Jun. 22, 2022.

For correspondence or reprints, contact Richard L. Wahl (rwahl@wustl.edu).

\*Contributed equally to this work.

Published online Jun. 30, 2022.

COPYRIGHT © 2023 by the Society of Nuclear Medicine and Molecular Imaging.

currently recommended by the American College of Radiology as an appropriate modality for indeterminate renal masses, largely due to the limited patient numbers in studies supporting its use (18).

Therefore, we conducted this study to assess the diagnostic accuracy of <sup>99m</sup>Tc-sestamibi SPECT/CT for characterization of solid renal lesions as concerning or nonconcerning, with histopathology as the reference standard, in patients who had undergone these scans for clinical indications. Secondary objectives included comparing the diagnostic performance of SPECT/CT with that of contrast-enhanced CT (ceCT), obtaining quantitative parameters on SPECT/CT, and estimating their optimal cutoffs for differentiating between concerning and nonconcerning renal lesions.

## MATERIALS AND METHODS

### Patients

Imaging and clinical records of patients who underwent <sup>99m</sup>Tc-sestamibi SPECT/CT for clinical evaluation of their solid renal lesions from September 2018 to October 2021 were retrospectively reviewed. Histopathology results obtained either from biopsy or after surgical excision of the lesions formed the reference standard. Patients with no histopathologic determination of their renal lesions were excluded from the study. The histopathologic diagnoses were categorized as malignant/concerning (RCCs other than chromophobe histology) or benign/nonconcerning (oncocytic renal neoplasms, chromophobe RCC, other benign diagnoses) to calculate the sensitivity and specificity of <sup>99m</sup>Tc-sestamibi SPECT/CT and ceCT. Considering that most benign or nonconcerning neoplasms such as oncocytoma are positive on <sup>99m</sup>Tc-sestamibi SPECT/CT, the sensitivity and specificity of both SPECT/CT and ceCT for the diagnosis of a nonconcerning neoplasm were calculated. Thus, the nonconcerning lesions were regarded as positive and concerning lesions were regarded as negative for estimation of the diagnostic accuracy of SPECT/CT and ceCT.

### <sup>99m</sup>Tc-Sestamibi SPECT/CT

The patients fasted for approximately 6 h before radiotracer injection, drank about 500 mL of plain water before the study, and were injected intravenously with about 925 MBq (25 mCi) of <sup>99m</sup>Tc-sestamibi. Approximately 75 min after the injection, SPECT/CT of the abdomen was performed with the kidneys in the center of the long-axis field of view. A SPECT/CT camera with a low-energy high-resolution collimator was used for imaging. The SPECT images were acquired with a dual head using 3° stops in a 360° clockwise rotation, at a rate of 10 s per frame and in step-and-shoot mode. The matrix was 128 × 128. Low-dose CT images were acquired for attenuation correction. The SPECT/CT images were reconstructed in transaxial, sagittal, and coronal views and interpreted by an experienced nuclear medicine physician. The interpreting physician was aware of the clinical information and the other imaging findings.

Lesions with uptake similar to or higher than that of the background renal parenchyma were considered positive on <sup>99m</sup>Tc-sestamibi SPECT/CT, whereas lesions with negligible uptake, significantly lower than that of the background renal parenchyma, were considered negative. Parameters such as lesion size, wall thickening, attenuation (Hounsfield units [HU]), enhancement, internal septation, presence of fat, and calcification were considered in the interpretation of the ceCT images. The clinical reads of both ceCT and SPECT/CT were utilized for the visual classification of the renal masses. Additionally, the SPECT/CT images were manually segmented to obtain maximum and mean counts of the lesion and adjacent renal cortex, as well as lesion maximum HU (HU<sub>max</sub>) and mean HU (HU<sub>mean</sub>). Whole-lesion volumes of interest were used to calculate lesion counts and HU. To measure the renal counts, a fixed 1.5-cm-diameter spheric volume of interest was placed in the adjacent renal cortex, avoiding areas of high radiotracer activity (e.g., the pelvicalyceal system). The lesion-to-kidney maximum and mean count ratios (LK<sub>max</sub> and LK<sub>mean</sub>, respectively) were calculated.

**TABLE 1**

Demographic and Clinical Data of Study Participants

Parameter	Data
Patients (n)	27 (male, 18; female, 9)
Age (y)	68 (58.5–77)
Histopathologic analysis procedure	Surgical histopathology, 23 (partial nephrectomy, 17; radical nephrectomy, 6); biopsy, 4
Renal lesions with histopathology (n)*	Total, 36 (100%)
	≤4 cm, 21 (58.3%)
	>4, ≤7 cm, 13 (36.1%)
	>7, ≤10 cm, 2 (5.5%)
Maximum dimension of lesion (cm)	3.3 (2.07–4.57)
Tumor laterality	Left, 19 (52.8%); right, 17 (47.2%)
Days between ceCT and SPECT/CT	30 (19.5–70.5)

\*Stratified by maximum dimension.  
Qualitative data are number and percentage; continuous data are median and interquartile range.

**TABLE 2**

Histopathologic Diagnosis of Renal Lesions Stratified by Size on Imaging

Histologic type	Maximum axial dimension on imaging		
	≤4 cm (n = 21)	>4, ≤7 cm (n = 13)	>7, ≤10 cm (n = 2)
<b>Concerning</b>			
Clear cell RCC	6 (28.6%)	6 (46.1%)	1 (50%)
Papillary RCC	4 (19%)	1 (7.7%)	0 (0%)
Collision clear cell, chromophobe RCC	0 (0%)	1 (7.7%)	0 (0%)
<b>Nonconcerning</b>			
Oncocytoma	4 (19%)	1 (7.7%)	1 (50%)
Chromophobe RCC	1 (4.8%)	1 (7.7%)	0 (0%)
Hybrid oncocytic chromophobe tumor	1 (4.8%)	1 (7.7%)	0 (0%)
Oncocytic renal neoplasm	3 (14.3%)	1 (7.7%)	0 (0%)
RCC with oncocytic features	0 (0%)	1 (7.7%)	0 (0%)
Angiomyolipoma	2 (9.5%)	0 (0%)	0 (0%)



**FIGURE 1.** A 53-y-old woman with right interpolar mass underwent MRI that suggested oncocytoma or chromophobe RCC.  $^{99m}\text{Tc}$ -sestamibi SPECT/CT was performed 1 wk later. Axial SPECT (A), CT (B), and SPECT/CT (C) images showed exophytic renal mass in right interpolar region (arrow) with negligible uptake that was suggestive of RCC. Patient underwent right partial robot-assisted laparoscopic nephrectomy, and histopathology was consistent with papillary RCC (World Health Organization/International Society of Urologic Pathologists grade 2).

### Statistical Analysis

The quantitative parameters ( $LK_{\max}$ ,  $LK_{\text{mean}}$ ,  $HU_{\max}$ , and  $HU_{\text{mean}}$ ) were tested for significant differences between concerning and nonconcerning lesions. Multiple logistic regression was used to build a model containing variables significant on univariate analyses. Receiver-operating-characteristic curves were drawn to estimate the performance of quantitative SPECT. The receiver-operating-characteristic curves for visual and quantitative  $^{99m}\text{Tc}$ -sestamibi SPECT/CT and ceCT were compared using the method of Hanley. The Mann-Whitney  $U$  test (2-tailed) was used to compare continuous variables between the visually characterized concerning and nonconcerning lesion groups. The Fisher exact test was used to compare categorical variables between the 2 groups. The diagnostic accuracy of SPECT/CT and ceCT was expressed as sensitivity and specificity. A  $P$  value of less than 0.05 was regarded as significant.

The retrospective review was approved by the institutional review board, and the need for written informed consent was waived.

### RESULTS

$^{99m}\text{Tc}$ -sestamibi was performed on 42 patients to evaluate their 62 renal lesions. Twenty-seven patients (18 male, 9 female) with 36 renal lesions had a final histopathologic diagnosis by either surgery ( $n = 23$ ) or biopsy ( $n = 4$ ). Twenty of these patients also

had ceCT. Most renal lesions (58.3%) were no more than 4 cm in maximal axial dimension. Table 1 shows the clinical and demographic data of the study participants. The initial detection of the renal lesions was incidental in 21 of 27 (77.8%) patients (19, CT of abdomen and pelvis; 2, MRI of abdomen).

Histopathology results showed 19 concerning (52.8%) and 17 nonconcerning (47.2%) diagnoses (Table 2). Overall, clear cell RCC was the most commonly identified single histologic type (13/36; 36.1%). As a group, oncocytic renal neoplasms (15/36; 41.6%) were most commonly diagnosed. The per-lesion test yield for providing a conclusive diagnosis (either true or false) was 84.6% (22/26) for CECT and 94.4% (34/36) for SPECT/CT. Two lesions were most likely too small to be adequately characterized on  $^{99m}\text{Tc}$ -sestamibi SPECT/CT (maximal axial dimension, 0.8 cm and 1.5 cm, with a final diagnosis of oncocytic renal neoplasm and chromophobe RCC, respectively). Of the 4 lesions for which the ceCT findings were inconclusive, 3 were correctly diagnosed (2 oncocytoma, 1 ccRCC) and 1 was false-positive (ccRCC on histopathology) on SPECT/CT.

Nine of 15 (60%) oncocytic renal neoplasms showed uptake visually on  $^{99m}\text{Tc}$ -sestamibi SPECT/CT and were correctly identified, whereas none (of the 10 masses with ceCT results) were correctly identified as nonconcerning on ceCT. Four oncocytic renal neoplasms were incorrectly identified as concerning on SPECT/CT. Twelve of 13 ccRCCs (92.3%) showed no uptake on  $^{99m}\text{Tc}$ -sestamibi SPECT/CT and were correctly classified as concerning, whereas ceCT correctly classified 80% of these lesions (8/10 with ceCT results).  $^{99m}\text{Tc}$ -sestamibi SPECT/CT could correctly classify 80% of the papillary RCCs (Fig. 1), compared with 33.3% on ceCT. A patient with a collision tumor (clear cell and chromophobe RCC) was correctly classified on SPECT/CT and misclassified as oncocytoma on ceCT (Fig. 2). Table 3 shows the distribution of tumor histologic types and their correctly identified proportions on  $^{99m}\text{Tc}$ -sestamibi SPECT/CT and ceCT.

Among the quantitative parameters,  $LK_{\text{mean}}$  and  $LK_{\max}$  were significantly higher in the nonconcerning lesions than in the concerning lesions (median  $LK_{\text{mean}}$ , 0.79 vs. 0.26,  $P < 0.001$ ; median  $LK_{\max}$ , 0.95 vs. 0.48,  $P = 0.005$ ), whereas the median  $HU_{\max}$  was significantly lower in the nonconcerning lesions (69 vs. 90.5,  $P = 0.01$ ) (Table 4). There was no significant difference in lesion size or  $HU_{\text{mean}}$  between concerning and nonconcerning lesions. Receiver-operating-characteristic curve analysis determined an optimal cutoff of 0.64 for  $LK_{\max}$  (area under the curve [AUC], 0.79; 95% CI, 0.61–0.92;  $P < 0.01$ ) and 0.46 for  $LK_{\text{mean}}$  (AUC, 0.85; 95% CI, 0.67–0.95;  $P < 0.0001$ ) for detecting nonconcerning lesions. There was no significant difference in the AUC of  $LK_{\max}$ - and  $LK_{\text{mean}}$ -based classifiers ( $P = 0.18$ ). Multiple logistic regression was used to analyze the relationship between  $LK_{\text{mean}}$ ,

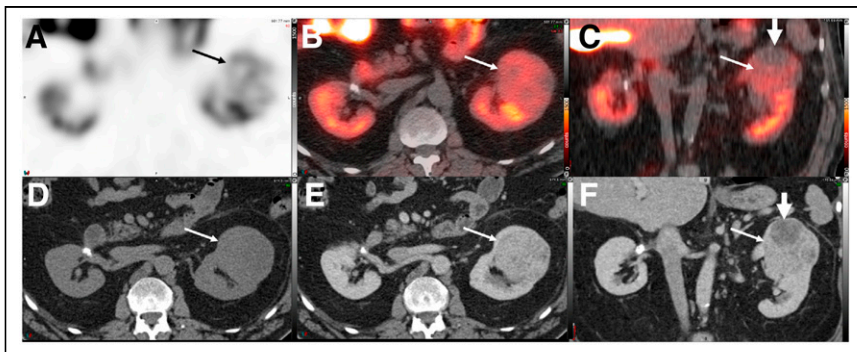


**FIGURE 2.** A 67-y-old man with previously diagnosed right RCC after right partial nephrectomy presented with enlarging left renal mass.  $^{99m}\text{Tc}$ -sestamibi axial SPECT (A) and SPECT/CT (axial, B; coronal, C) images show mass in superior pole of left kidney, with inferior part showing tracer avidity (thin arrow) and superior part showing relative photopenia (thick arrow). It was diagnosed as likely collision tumor on SPECT/CT, with inferior, tracer-avid region likely representing oncocytic tumor and superior, photopenic region likely representing RCC. ceCT images (noncontrast, D; postcontrast nephrogenic phase axial, E; coronal, F) showed solid, heterogeneously enhancing left renal mass likely representing oncocytoma. Patient underwent left partial robot-assisted laparoscopic nephrectomy, and histopathology showed collision tumor composed of clear cell RCC (rhabdoid differentiation, World Health Organization/International Society of Urologic Pathologists grade 4) and eosinophilic variant of chromophobe RCC.

**TABLE 3**

Distribution of Tumor Histologies and Their Correctly Identified Proportions on <sup>99m</sup>Tc-Sestamibi SPECT/CT and ceCT

Histologic type	Histopathology (n)	Correct diagnosis (n)	
		<sup>99m</sup> Tc-sestamibi SPECT/CT	ceCT*
<b>Concerning</b>			
Clear cell RCC	13 (36.1%)	12 (92.3%)	8/10 (80%)
Papillary RCC	5 (13.9%)	4 (80%)	1/3 (33.3%)
Collision clear cell, chromophobe RCC	1 (2.8%)	1 (100%)	0/1 (0%)
<b>Nonconcerning</b>			
Oncocytoma	6 (16.7%)	3 (50%)	0/4 (0%)
Chromophobe RCC	2 (5.5%)	1 (50%)	0/2 (0%)
Hybrid oncocytic chromophobe tumor	2 (5.5%)	2 (100%)	0/0 (0%)
Oncocytic renal neoplasm	4 (11.1%)	2 (50%)	0/3 (0%)
RCC with oncocytic features	1 (2.8%)	1 (100%)	0/1 (0%)
Angiomyolipoma	2 (5.5%)	1 (50%)	1/2 (50%)

\*Data are for when ceCT was performed.

HU<sub>max</sub>, and detection of a nonconcerning lesion. The odds of detecting a nonconcerning lesion were higher with increasing LK<sub>mean</sub> (odds ratio, 271.65; 95% CI, 5.28–13,981.9; *P* = 0.005) and decreasing HU<sub>max</sub> (odds ratio, 0.93; 95% CI, 0.87–0.99; *P* = 0.019). The combination of these 2 quantitative measurements on logistics regression yielded an AUC of 0.92 (95% CI, 0.76–0.99). Visually interpreted <sup>99m</sup>Tc-sestamibi SPECT/CT had a sensitivity and specificity of 66.7% (95% CI, 38.4–88.2) and 89.5% (95% CI, 66.7–98.7), respectively. This was not significantly different from the performance of ceCT (Table 5; Supplemental Fig. 1; supplemental materials are available at <http://jnm.snmjournals.org>). However, quantitative SPECT/CT (based on an LK<sub>mean</sub> cutoff of 0.46 for a nonconcerning lesion; Supplemental Fig. 2) performed significantly better (AUC, 0.85; 95% CI, 0.62–0.96) than ceCT (AUC, 0.57; 95% CI, 0.34–0.78), with a *P* value of 0.023.

**DISCUSSION**

On visual interpretation, <sup>99m</sup>Tc-sestamibi SPECT/CT correctly identified 89.5% of all aggressive tumors and 60% of all oncocytic neoplasms in our study. The false-positive results (a concerning

lesion labeled as nonconcerning) stemmed from tracer avidity in 2 concerning lesions that were positive based on the quantitative criteria as well (clear cell RCC with LK<sub>mean</sub> of 1.17 and papillary RCC with LK<sub>mean</sub> of 0.82). A few prior studies have also shown that a limited number of papillary and clear cell RCC cases may show uptake of <sup>99m</sup>Tc-sestamibi (14,16). This is likely related to a higher contribution from the mitochondrial content of these tumors and a relatively lower expression of the multidrug resistance protein. Although a prior study showed that papillary RCC has a uniformly increased expression of multidrug resistance protein in comparison to mitochondrial content, this might not hold true in a larger cohort (12).

The visual detection rate of nonconcerning lesions on <sup>99m</sup>Tc-sestamibi SPECT/CT was lower in our study than in the prior studies. One possible reason is the relatively higher number of benign or nonconcerning lesions included in our study (~47%) than in the prior ones (~24%) (15–17). Because of the higher number of nonconcerning lesions, we could report that oncocytomas may not universally show high uptake on <sup>99m</sup>Tc-sestamibi SPECT/CT and can be missed on both visual and quantitative assessment (Fig. 3). However, in 2 of the 3 cases in which visual assessment was false-negative and

**TABLE 4**

Comparison of Quantitative Parameters on <sup>99m</sup>Tc-Sestamibi SPECT/CT for Differentiating Clinically Concerning from Nonconcerning Renal Lesions

Parameter	Concerning lesions	Nonconcerning lesions	<i>P</i>
Lesional maximal axial dimension (cm)	3.3 (2.3–4.8)	2.95 (1.47–4.62)	0.386
LK <sub>max</sub>	0.48 (0.37–0.64)	0.95 (0.69–1.04)	0.005
LK <sub>mean</sub>	0.26 (0.12–0.43)	0.79 (0.55–0.99)	<0.001
Lesion HU <sub>max</sub>	90.5 (78–101)	69 (60.5–89.5)	0.016
Lesion HU <sub>mean</sub>	26.25 (22.98–31.75)	28.1 (23.55–31.0)	0.801

Data are median and interquartile range.



**TABLE 5**

Comparison of Diagnostic Accuracy of <sup>99m</sup>Tc-Sestamibi SPECT/CT and ceCT for Diagnosing Nonconcerning Renal Lesions

Diagnostic modality	TP (n)	TN (n)	FP (n)	FN (n)	Sensitivity	Specificity
<sup>99m</sup> Tc-sestamibi SPECT/CT: visual interpretation	10	17	2	5	66.7 (0.38–0.88)	89.47 (0.67–0.99)
ceCT	1	9	3	9	10.0 (0.25–0.44)	75.0 (0.43–0.95)
<sup>99m</sup> Tc-sestamibi SPECT/CT: LK <sub>mean</sub> *	14	13	2	2	87.5 (0.62–0.98)	86.67 (0.59–0.98)

\*Using cutoff value of LK<sub>mean</sub> > 0.46 for nonconcerning lesion.

TP = true-positive; TN = true-negative; FP = false-positive; FN = false-negative.

Nonconcerning lesions are positive, and concerning lesions are negative. Data in parentheses are 95% CI.

quantitative assessment was performed, the latter was able to make the correct diagnosis. Since the pattern of uptake can vary widely in oncocyctic tumors, ranging from homogeneously increased uptake compared with the normal renal parenchyma to areas of low-grade patchy uptake with interspersed photopenia, quantitative assessment with the lesion-to-background count ratios can complement visual interpretation (19).

Most prior studies used either visual interpretation alone or a combination of visual interpretation with LK<sub>max</sub>. Our LK<sub>max</sub> cutoff of 0.64 for detecting nonconcerning lesions is similar to that reported previously, validating the utility of this quantitative criterion (11,20). We additionally introduced LK<sub>mean</sub>, which is more reflective of the count distribution in the entire tumor than are the total counts in a heterogeneous lesion. We also propose combining HU<sub>max</sub> and LK<sub>mean</sub> on SPECT/CT; this combination showed a higher AUC, 0.92 (95% CI, 0.76–0.99), than did the other quantitative parameters alone on the receiver-operating-characteristic analyses. Although this method did not significantly differ from using LK<sub>mean</sub> alone, the lack of significance is quite possibly related to the relatively low number of lesions included in this study. The use of quantitative parameters from both SPECT and CT components has not, to our knowledge, been explored before and needs validation in future prospective studies. The prospects of performing a single <sup>99m</sup>Tc-sestamibi SPECT/ceCT study may also be explored as a 1-stop shop for evaluation of renal masses (21), reducing the number of patient visits and potentially improving interpretation of renal masses by combining features from both SPECT and ceCT.

It is recognized that conventional imaging such as CT and MRI often detects renal lesions incidentally but cannot reliably distinguish indolent renal tumors from aggressive ones. In our study, 9 of 15 oncocyctic lesions were correctly identified on SPECT/CT, whereas none could be accurately categorized on ceCT. Although the difference in the sensitivity and specificity of visually interpreted SPECT/CT and ceCT was not statistically significant, this lack of significance was likely due to the limited number of lesions studied by both modalities. The incremental value of SPECT/CT in detecting oncocyctic lesions is clinically relevant and can potentially avoid overtreatment in these patients. A prior study has shown that addition of <sup>99m</sup>Tc-sestamibi SPECT/CT after conventional imaging increases diagnostic confidence and improves accuracy in differentiating benign from malignant tumors (20). Further, <sup>99m</sup>Tc-sestamibi SPECT/CT followed by biopsy to confirm benign small renal masses is reported to be a cost-effective strategy with the highest probability of not overtreating benign tumors and appropriately treating malignant ones (22).

Our study had its limitations. These included a retrospective design with a limited number of participants, leading to wide 95% CIs in estimates of diagnostic accuracy, although we had several unique histologic types for which we could show differences in performance between ceCT and <sup>99m</sup>Tc-sestamibi SPECT/CT. The diagnostic accuracy of both ceCT and <sup>99m</sup>Tc-sestamibi SPECT/CT is possibly underestimated because of the retrospective design, in which SPECT/CT was more likely to be performed in challenging cases with lack of a reliable, conclusive diagnosis on ceCT. Nevertheless, the literature is still quite sparse in this space in terms of original articles describing findings in unique populations (11,13–16).

Our exclusion of patients with no histopathology results might have led to selective exclusion of a higher number of benign or nonconcerning lesions that were more likely to be managed clinically by follow-up imaging instead of active intervention. We hope to follow up our patients to determine how many lesions were stable over time without intervention. However, our stringent inclusion criteria with histopathology as the reference standard helped form a robust comparison for both ceCT and SPECT/CT. Additionally, most patients in our study had surgical histopathology results, thereby minimizing the potential inconclusive or false results with a biopsy. Instead of central reads, we incorporated both clinical visual reads and quantitative results for SPECT/CT, which

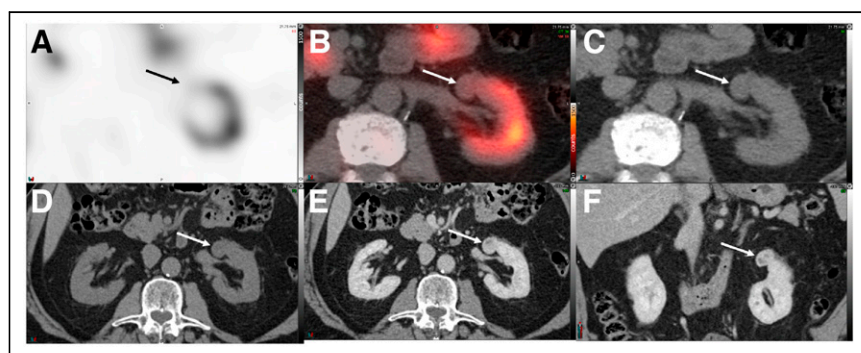


**FIGURE 3.** A 77-year-old man presented with left renal mass. <sup>99m</sup>Tc-sestamibi axial SPECT (A), SPECT/CT (B) and CT (C) images showed exophytic mass in anterior interpolar region of left kidney (arrow) with negligible uptake, likely representing RCC. LK<sub>max</sub> and LK<sub>mean</sub> were both 0.3 for this lesion. ceCT images (axial noncontrast, D; postcontrast nephrogenic phase, E; coronal, F) showed enhancement in mass and also suggested diagnosis of RCC. Patient underwent left partial robot-assisted laparoscopic nephrectomy, and histopathology was consistent with oncocytoma.

likely better reflects the real-world scenario. The cutoffs for mean and maximum count ratio between the lesions and the normal renal parenchyma were set post hoc, and these would need prospective validation in larger cohorts. Importantly, we combined the quantitative information from SPECT and CT, in terms of count ratios and  $HU_{max}$ , which performed better than either of these parameters alone. Future prospective studies can focus on use of these parameters along with visual reads to improve the diagnostic accuracy of  $^{99m}Tc$ -sestamibi SPECT/CT.

## CONCLUSION

The current literature on the utility of  $^{99m}Tc$ -sestamibi SPECT/CT for characterization of solid renal masses is limited, with a recently published systematic review reporting only 4 studies. We provide additional evidence of the utility of  $^{99m}Tc$ -sestamibi SPECT/CT, especially in patients with an inconclusive ceCT result for differentiating malignant or aggressive renal tumors from benign or indolent ones, therefore potentially avoiding overtreatment and its associated complications in the latter category. Quantitative assessment can further increase the diagnostic accuracy of SPECT/CT and may be used in conjunction with visual interpretation.

## DISCLOSURE

No potential conflict of interest relevant to this article was reported.

## KEY POINTS

**QUESTION:** What is the diagnostic accuracy of  $^{99m}Tc$ -sestamibi SPECT/CT for solid renal lesions?

**PERTINENT FINDINGS:** In this retrospective study, we showed that  $^{99m}Tc$ -sestamibi SPECT/CT had a sensitivity and specificity of 66.7% and 89.5%, respectively, for diagnosing a nonconcerning solid renal lesion.

**IMPLICATIONS FOR PATIENT CARE:** The study showed that  $^{99m}Tc$ -sestamibi SPECT/CT can aid in the diagnosis of solid renal lesions, especially when the ceCT results are inconclusive.

## REFERENCES

1. Welch HG, Skinner JS, Schroeck FR, Zhou W, Black WC. Regional variation of computed tomographic imaging in the United States and the risk of nephrectomy. *JAMA Intern Med.* 2018;178:221–227.
2. Silverman SG, Israel GM, Herts BR, Richie JP. Management of the incidental renal mass. *Radiology.* 2008;249:16–31.
3. Frank I, Blute ML, Cheville JC, Lohse CM, Weaver AL, Zincke H. Solid renal tumors: an analysis of pathological features related to tumor size. *J Urol.* 2003;170:2217–2220.
4. Sanchez A, Feldman AS, Ari Hakimi A. Current management of small renal masses, including patient selection, renal tumor biopsy, active surveillance, and thermal ablation. *J Clin Oncol.* 2018;36:3591–3600.
5. Pierorazio PM, Johnson MH, Ball MW, et al. Five-year analysis of a multi-institutional prospective clinical trial of delayed intervention and surveillance for small renal masses: the DISSRM registry. *Eur Urol.* 2015;68:408–415.
6. Jewett MAS, Richard PO, Finelli A. Management of small renal mass: an opportunity to address a growing problem in early stage kidney cancer. *Eur Urol.* 2015;68:416–417.
7. Finelli A, Ismaila N, Bro B, et al. Management of small renal masses: American Society of Clinical Oncology clinical practice guideline. *J Clin Oncol.* 2017;35:668–680.
8. Menoguz SR, O'Brien BA, Brown AL, Cohen RJ. Percutaneous core biopsy of small renal mass lesions: a diagnostic tool to better stratify patients for surgical intervention. *BJU Int.* 2013;111:E146–E151.
9. Leveridge MJ, Finelli A, Kachura JR, et al. Outcomes of small renal mass needle core biopsy, nondiagnostic percutaneous biopsy, and the role of repeat biopsy. *Eur Urol.* 2011;60:578–584.
10. Ball MW, Bezerra SM, Gorin MA, et al. Grade heterogeneity in small renal masses: potential implications for renal mass biopsy. *J Urol.* 2015;193:36–40.
11. Gorin MA, Rowe SP, Baras AS, et al. Prospective evaluation of  $^{99m}Tc$ -sestamibi SPECT/CT for the diagnosis of renal oncocytomas and hybrid oncocytic/chromophobe tumors. *Eur Urol.* 2016;69:413–416.
12. Rowe SP, Gorin MA, Solnes LB, et al. Correlation of  $^{99m}Tc$ -sestamibi uptake in renal masses with mitochondrial content and multi-drug resistance pump expression. *EJNMMI Res.* 2017;7:80.
13. Rowe SP, Gorin MA, Gordetsky J, et al. Initial experience using  $^{99m}Tc$ -MIBI SPECT/CT for the differentiation of oncocytoma from renal cell carcinoma. *Clin Nucl Med.* 2015;40:309–313.
14. Tzortzakakis A, Gustafsson O, Karlsson M, Ekström-Ehn L, Ghaffarpour R, Axelsson R. Visual evaluation and differentiation of renal oncocytomas from renal cell carcinomas by means of  $^{99m}Tc$ -sestamibi SPECT/CT. *EJNMMI Res.* 2017;7:29.
15. Sistani G, Bjazevic J, Kassam Z, Romsa J, Pautler S. The value of  $^{99m}Tc$ -sestamibi single-photon emission computed tomography-computed tomography in the evaluation and risk stratification of renal masses. *Can Urol Assoc J.* 2021;15:197–201.
16. Zhu H, Yang B, Dong A, et al. Dual-phase  $^{99m}Tc$ -MIBI SPECT/CT in the characterization of enhancing solid renal tumors: a single-institution study of 147 cases. *Clin Nucl Med.* 2020;45:765–770.
17. Wilson MP, Katlariwala P, Murad MH, Abele J, McInnes MDF, Low G. Diagnostic accuracy of  $^{99m}Tc$ -sestamibi SPECT/CT for detecting renal oncocytomas and other benign renal lesions: a systematic review and meta-analysis. *Abdom Radiol (NY).* 2020;45:2532–2541.
18. Wang ZJ, Nikolaidis P, Khatri G, et al. ACR Appropriateness Criteria® indeterminate renal mass. *J Am Coll Radiol.* 2020;17:S415–S428.
19. Campbell SP, Tzortzakakis A, Javadi MS, et al.  $^{99m}Tc$ -sestamibi SPECT/CT for the characterization of renal masses: a pictorial guide. *Br J Radiol.* 2018;91:20170526.
20. Sheikhabaei S, Jones CS, Porter KK, et al. Defining the added value of  $^{99m}Tc$ -MIBI SPECT/CT to conventional cross-sectional imaging in the characterization of enhancing solid renal masses. *Clin Nucl Med.* 2017;42:e188–e193.
21. Israel O, Pellet O, Biassoni L, et al. Two decades of SPECT/CT: the coming of age of a technology—an updated review of literature evidence. *Eur J Nucl Med Mol Imaging.* 2019;46:1990–2012.
22. Su ZT, Patel HD, Huang MM, et al. Cost-effectiveness analysis of  $^{99m}Tc$ -sestamibi SPECT/CT to guide management of small renal masses. *Eur Urol Focus.* 2021;7:827–834.